INTERFACE

royalsocietypublishing.org/journal/rsif

Research

Cite this article: Le Pabic C, Derr J, Luquet G, Lopez P-J, Bonnaud-Ponticelli L. 2019 Three-dimensional structural evolution of the cuttlefish *Sepia officinalis* shell from embryo to adult stages. *J. R. Soc. Interface* **16**: 20190175. http://dx.doi.org/10.1098/rsif.2019.0175

Received: 14 March 2019
Accepted: 5 August 2019

Subject Category:
Life Sciences–Physics interface

Subject Areas:
biophysics, evolution, biomaterials

Keywords:
cuttlefish, shell, three-dimensional structure, tomography, development, buoyancy

Author for correspondence:
Laure Bonnaud-Ponticelli
e-mail: laure.bonnaud@mnhn.fr

Electronic supplementary material is available online at https://doi.org/10.6084/m9.figshare.c.4614917.

THE ROYAL SOCIETY PUBLISHING

Three-dimensional structural evolution of the cuttlefish *Sepia officinalis* shell from embryo to adult stages

Charles Le Pabic[1], Julien Derr[2], Gilles Luquet[1], Pascal-Jean Lopez[1] and Laure Bonnaud-Ponticelli[1]

[1]Unité Biologie des organismes et écosystèmes aquatiques (BOREA), Muséum national d'Histoire naturelle, UMR CNRS 7208, Université de Caen Normandie, Sorbonne Université, IRD 207, Université des Antilles, 75005 Paris, France
[2]Laboratoire Matière et Systèmes Complexes (MSC), Université Paris Diderot, UMR CNRS 7057, 75205 Paris Cedex 13, France

JD, 0000-0002-7965-3973; LB-P, 0000-0001-7510-5032

The cuttlefish shell is an internal structure with a composition and general organization unique among molluscs. Its formation and the structure–function relation are explored during *Sepia officinalis* development, using computerized axial tomography scanning (CAT-scan) three-dimensional analyses coupled to physical measurements and modelling. In addition to the evolution of the overall form, modifications of the internal structure were identified from the last third embryonic stages to adult. Most of these changes can be correlated to life cycle stages and environmental constraints. Protected by the capsule during embryonic life, the first internal chambers are sustained by isolated pillars formed from the dorsal to the ventral septum. After hatching, the formation of pillars appears to be a progressive process from isolated points to interconnected pillars forming a wall-delineated labyrinthine structure. We analysed the interpillar space, the connectivity and the tortuosity of the labyrinth. The labyrinthine pillar network is complete just prior to the wintering migration, probably to sustain the need to adapt to high pressure and to allow buoyancy regulation. At that time, the connectivity in the pillar network is compensated by an increase in tortuosity, most probably to reduce liquid diffusion in the shell. Altogether these results suggest adjustment of internal calcified structure development to both external forces and physiological needs.

1. Introduction

The external calcified shell of molluscs has been selected for its protective functions against predators and/or resistance against stressful physico-chemical factors. The cephalopods are the only molluscs building a chambered shell (phragmocone) used as a buoyant system [1], giving them an adaptive advantage in aquatic environment. Extinct ammonites and present nautiloids show an external chambered shell. During evolution, the external shell has been reduced and internalized in some lineages of cephalopods. As a consequence, behavioural, anatomical and physiological adaptations had to be selected to compensate the loss of the external protective function. In some groups of cephalopods, the internal chambered shell is strongly mineralized with mechanical but also physiological roles as in extinct belemnites, the closest relatives of present lineages, and two present groups of cephalopods: spirulids and sepiids. The sepiid shell, called the cuttlebone, presents numerous differences from that of nautiloids and spirulids. These latter organisms build spiral shells with about 30 large chambers, delimited by septa, filled with gas and liquid via a median tubular structure (the siphuncle) passing through the chambers. On the contrary, in sepiids, the shell is flat and formed of 100 thin chambers separated by septa, all opened posteriorly, where gas/liquid exchanges are regulated through this opened posterior area called siphuncular zone [1,2]. Moreover, each sepiid chamber is supported inside by vertical elements called 'pillars', spread over the entire septal surface and forming a complex labyrinthine structure

Table 1. Sample keys and age data of *Sepia officinalis* shells used in this study.

sample key	age	shell length (mm)	shell width (mm)	width/length ratio
MNHN-IM-2012-36001	embryonic stage 27	3.5	2.1	0.60
MNHN-IM-2012-36006	embryonic stage 30	6.0	3.5	0.58
MNHN-IM-2012-13923	one month	11.0	5.7	0.52
MNHN-IM-2012-13925	three months	33.2	13.0	0.39
MNHN-IM-2012-13927	18 months?	218.4	68.7	0.31

unique in cephalopods, the so-called pillar network [3,4]. Some hypotheses about spatial organization and organo-mineral formation of this pillar network have been previously proposed for *Sepia* shells [4–9], but with little investigation at the spatial and temporal scales. Yet, such a peculiar structuration should be considered in relation to physiological needs of the organism. Here, we have chosen to study the *Sepia officinalis* shell during its life cycle, from embryo to adult, with a special emphasis on spatio-temporal evolution of the pillar network, i.e. inside the same chamber and in different chambers of the same shell. Using computerized axial tomography scanning (CAT-scan) three-dimensional observations coupled with physical measurements and mathematical analyses, we describe the shell synthesis sequence and the global inside structure of cuttlefish shell, from embryonic to adult stages. Our results, associated with knowledge about the *S. officinalis* ecology, allow us to link shell structure with cuttlefish life stages and to hypothesize about the labyrinthine pillar network role in the cuttlefish shell buoyancy function, an essential prerequisite to further evolutionary studies.

2. Material and methods

2.1. Research specimens

The lengths, ages and sample keys of the five *S. officinalis* shells used in this study are indicated in table 1. All animals come from the English Channel and are at different ontogenic stages. In order to determine precisely their stage of development, they were reared at the Centre de Recherches en Environnement Côtier (Luc-sur-Mer, France) allowing a day-to-day follow up except for the adult stage (i.e. specimen MNHN IM-2012-13927) that was trawl-fished. Embryonic stages were determined according to the development table from Lemaire [10]: the shell begins to form at stage 25, when the embryo resembles an adult and the chambers appear progressively until hatching at stage 30.

During egg and juvenile rearing, water parameters were kept at 17 ± 1°C, 32.5 ± 1 psu (salinity) and less than 0.5 mg l^{-1} for ammonia- and nitrite-nitrogen and less than 80 mg l^{-1} for nitrate-nitrogen [11]. Juveniles were fed once a day with live brown shrimps *Crangon crangon* during all their maintenance. Before shell removal, cleaning and storage in 70% ethanol, animals (i.e. embryo and juveniles) were euthanized by 10% ethanol exposure during 10 min followed by cephalopodium (i.e. head, arms and funnel) removal [12,13]. The specimens MNHN IM-2012-36001 and MNHN IM-2012-36006 are both embryonic shells corresponding, respectively, to the beginning, stage 27, and to the end, stage 30, of the embryonic shell formation. According to the strong influence of food supply and temperature on the *S. officinalis* shell growth [14,15], the choice of the juvenile shells MNHN IM-2012-13923 (one-month old) and MNHN IM-2012-13925 (three-month old) were considered as the best compromise to study shell formation during the juvenile life period. The adult cuttlebone for scanning electron microscopy (SEM) analysis comes from specimen freshly fished along the English Channel coastline.

2.2. X-ray tomography

For the five *S. officinalis* shells, a high-resolution CAT-scan was acquired at the Platform AST-RX of the Museum National d'Histoire Naturelle (MNHN). In order to keep similar resolution in the first built chambers, a second CAT-scan was acquired for the specimen MNHN IM-2012-13925 (three-month old) focusing on the 15 first chambers of this shell. Data relative to this scan are bracketed here below next to the whole shell scan of the same specimen. The scanning parameters were, respectively, for the specimens IM-2012-36001 (stage 27), IM-2012-36006 (stage 30), MNHN IM-2012-13923 (one month), MNHN IM-2012-13925 (three months) and IM-2012-13927 (adult): an effective energy of 70, 70, 65, 55 (68) and 80 kV, a current of 180, 215, 250, 310 (275) and 300 mA, a voxel size 2.09, 3.36, 6.17, 18.25 (6.32) and 116.52 µm, and a view number of 2500, 3000, 1800, 1500 (3000) and 1200. Images were reconstructed and exported into 16-bit TIFF stacks using ImageJ 2.0.0 and Avizo Lite 9.0.1 softwares.

2.3. Scanning electron microscopy

In order to compare images resulting from CAT-scan and microscopy, small pieces of an adult *S. officinalis* cuttlebone (135-mm shell length) were prepared for optical microscopy and SEM observations. For SEM, cuttlebone pieces were mounted on SEM stubs and covered with a 10-nm gold layer through sputtering using a Jeol FJC-1200 metal coater. SEM observations were performed with a Hitachi SU 3500 microscope using the BSE (backscattered electron) mode.

2.4. Physical analysis of the inside shell pillar network

In order to perform repeatable and comparable height measurements (inside the same shell and between different shells), we set up the following methodology. Along the shell sagittal plane, we measured the greatest chamber height perpendicular to the bottom septa median plane (electronic supplementary material, figure S1). Except for the first synthesized chambers (of each shell), this measure is always located at the front extremity of the top chamber. Height measurements were made using ImageJ 2.0.0 software.

Because our observations of the inner parts in studied shells did not underline major structural differences between the same chambers of different shells, we chose the three-month-old shell for the work on the pillar network (i.e. connectivity, interpillar space and tortuosity). Each physical analysis has been made on every three-month shell chambers (i.e. from chamber 1, the first one built in embryo to chamber 34, the last chamber formed in the three-month shell). All image processing was done using the *scikit-image* Python package [16].

To determine whether the different inner chamber zones (i.e. space zones) are connected together, particularly in chambers with complex pillar network, we used standard image processing techniques [17,18], implemented in the *scikit-image* package [16], which enabled us to label a binary image by counting the connected regions. From that, we were able to draw a histogram of the size distribution of the different connected regions.

To estimate the pillar spacing, for each chamber, we cropped a region representative of the chamber (typically situated at the centre of the chamber) and used directly the cropped image in grayscale. We estimated the interpillar spacing by using a method based on auto-correlation as described in electronic supplementary material, figure S2. To access the typical space between pillars, we performed multiple times one-dimensional cut of the image. For each trial, starting and ending points were randomly picked in the image with the only condition that the length of the cut would be bigger than a minimum value (arbitrarily picked as half the minimum dimension of the cropped image). A greyscale one-dimensional profile was recorded along the cut. These one-dimensional profiles exhibited oscillations, but not long enough to efficiently perform Fourier transform. Instead, we chose a similar technique based on auto-correlation (J. Philippi 2019, personal communication). We computed the auto-correlation of the profile, and as the signal is roughly sinusoidal, the auto-correlation profile presents first a minimum when signals are in opposite phase and then a maximum when they are back in phase. Positions of the first local minimum and first local maximum gave two measurements of the same typical spatial period of the signal. To be sure that our trial is meaningful, we considered the measurement as valid if and only if the relative difference between the two measurements was less than 0.5%. Repeating the trials, we obtained, for each chamber, a distribution of measurements of the spatial period.

To describe the pillar network tortuosity, for each chamber, we used the same selection of images as described for pillar spacing measurements. We performed a binarization of the cropped image in greyscale using Otsu's method [19]. Then, we computed the corresponding topological skeleton: a 1-pixel wide skeleton of the object, with the same connectivity as the original object. Applying a generic filter on the skeleton enabled us to discriminate between segment pixels, edge pixels or crossing pixels. From there, one can transform the skeleton into a graph structure. For graph structures, classical Dijkstra's algorithm has been used to compute shortest path [20], i.e. to go from one point A to one point B. The tortuosity of this path is defined mathematically as the arc/chord ratio: the ratio of the length of the path $\widehat{AB}$ to the Euclidian distance $\overline{AB}$. The starting points and the ending points are randomly picked in the cropped image (following a uniform distribution). Tortuosity is computed for this path, and the operation is repeated a number of times to get statistics. For each chamber, we performed thousands of trials in order to get a standard error of typically less than 1%. Then, we performed the same analysis in segregating between horizontal and vertical orientation of the paths. We chose the simplest criteria: if the angle between the Euclidian path (starting to ending point) and the horizontal line was more than 45°, we defined it to be vertical, or horizontal if less than 45°.

To check the homogeneity of the results among one chamber (which is always bigger than the cropped probe area), we performed the same analysis on chamber 30 by shifting the probe area from −1 to 1 time its size.

3. Results

Cuttlebone grows by ventral accretion of chambers from the posterior to the anterior part of the shell during the whole cuttlefish life. Most of the time, the first synthesized chambers (i.e. embryonic) are neither observable nor accessible in adult shell (even young) because of the important growth and calcification of the animal during its life cycle (table 1).

3.1. Embryonic stages (i.e. 27 and 30)

The shells from stage 27 and stage 30 embryos are made up of three and six chambers, respectively (figure 1*a*; electronic supplementary material, figure S3), as previously observed [4–10]. Their heights range from 0.25 to 0.31 mm with a mean chamber height of 0.27 ± 0.02 and 0.28 ± 0.03 mm (mean ± s.d.) for stage 27 and stage 30 embryo shells, respectively (figure 2).

In both shells, we observe distinct pillars (i.e. disconnected from each other). The pillar shape and organization are different in the siphuncular area and in the plane-anterior area. In the first one, their density is higher, and they present in a large majority a straight cylindrical shape with bulging at their ventral side (figure 3*a*; electronic supplementary material, figure S4-movie). In the anterior area, their shapes are either cylindrical or elongated along the sagittal axis (figure 3). From dorsal to ventral septum, most of these pillars widen to finally form branches with an increase in tortuosity for the elongated pillars (figure 3*b*). The stage 27 shell X-ray tomography allowed us to observe the beginning of the fourth chamber build up process, with the dorsoventral growth of pillars prior to the septa floor formation. We also evidenced that the pillars are formed progressively from anterior to posterior: there is no pillar building in the same time on all the chamber surface (figure 3*a*; electronic supplementary material, figure S4-movie).

3.2. Juvenile stages (i.e. one- and three-month-old animals)

Juvenile shells from one- and three-month-old cuttlefish reared in controlled conditions are, respectively, made up of 19 and 34 chambers (electronic supplementary material, figure S3). Whereas absent from embryonic shells, the spine is clearly present in both juvenile shells highlighting the synthesis of this structure after hatching (electronic supplementary material, figure S3, arrowheads). The one-month-old shell scan allowed us to observe the formation of a new septum (figure 4). It appears that this chamber build up step occurs from the front to the back of the shell, similarly to the pillar formation described in §3.1.

The chamber heights range from 0.10 to 0.41 mm with a mean chamber height of 0.18 ± 0.07 and 0.27 ± 0.08 mm, for one- and three-month-old shell, respectively. These important variations (RSD = 39 and 30%, respectively) are due to chamber height decrease (below 0.20 mm) from chambers 8 to 12, observed in both shells (figure 2). Looking at the mineral structures inside of the chamber shell, from the dorsal to the ventral side of the shell, the width of the pillar increases and their tips mainly correspond to tortuous elongated lines in place of the branching described in embryonic chambers. This chamber-to-chamber change results in the progressive linkage of pillars forming a labyrinth network near the 25th shell chamber (figure 5; electronic supplementary material, figure S5-movie).

3.3. From embryo to adult: the growth of the shell

From an external view, the overall main dimensions of the shell increase. During the cuttlefish life cycle, the width/length ratio of the shell is divided by two (0.6–0.3; table 1), with important decrease between embryonic stages and three-month shell from 0.6 to 0.39. Our data are consistent with those of Sherrard obtained on three adult *S. officinalis* shells coming from Mediterranean Sea (average width/length ratio of 0.36 for an average shell length of 146 mm) [3]. The same author highlighted that such width/length ratio is significantly higher in adult shells coming from *Sepia* species living in shallow area (less than 100 m) than those living at greater depth (greater than 100 m), suggesting the shell surface importance to deal with higher

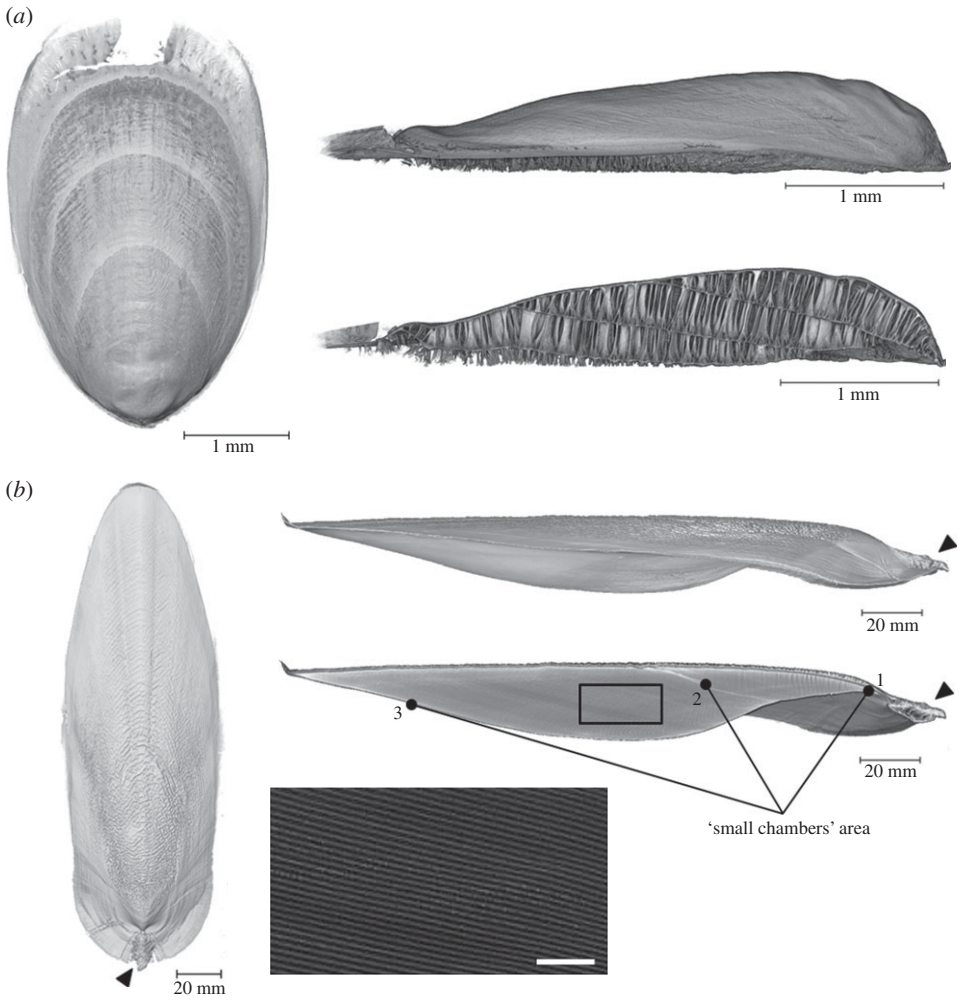

Figure 1. Three-dimensional images of (*a*) embryonic stage 27 and (*b*) adult cuttlefish shell. The growth allometry is clearly visible between embryo and adult. Arrowheads indicate the spine. The three 'small chambers' area indicated on adult shell corresponds to chambers too small and/or thin to be precisely counted and measured. The magnification panel of the adult shell scan highlights the shell septa. Scale bar: 5 mm.

pressure. According to this observation, we propose that this change of width/length ratio during the first months of life could be necessary to the *S. officinalis* migration in deeper waters during winter.

3.4. Adult stage

The CAT-scan resolution of the image of an adult shell (even if of important size: 218.4 mm; table 1) allowed us to determine that it is made up of more than 100 chambers. Among these chambers, it has been possible to measure 84 chamber heights (figure 2). The heights range from 0.17 to 0.43 mm with a mean chamber height of 0.33 ± 0.05 mm. We observed a progressive increase of the first chamber heights corresponding to the beginning of the juvenile stage (estimated to be from chambers 8 to 19; figure 2). The 16 (at least) other chambers were too small and/or thin to be precisely counted and measured (figure 1*b*). As a whole, three distinct areas of these 'small chambers' were identified in adult shell (from early to later stages of life): (1) the six first chambers (embryonic life), (2) from chambers 35 to 40 (at least), and (3) the three last synthesized chambers (at least).

3.5. Physical measurements and analyses

The analysis of the connectivity showed that the pillar network constitutes an almost unique space, whatever its complexity. Indeed, from chambers 15 to 34, we found connection values of the total chambers above 90% (figure 6).

Our analysis of the interpillar space evolution in the 34 first synthesized chambers (i.e. in three-month-old shell) highlighted three phases (figure 7).

Firstly, the values of interpillar space from chamber 1 (43.0 ± 4.8 µm) to chamber 9 (45.0 ± 4.9 µm) remains stable. Then, interpillar space values increase progressively until chamber 27 (108.8 ± 12.5 µm) to finish by a stable phase from chamber 28 (111.4 ± 13.7 µm) to chamber 34 (116.3 ± 22.9 µm) with mean values around 114.9 ± 2.4 µm. Notably, interpillar spaces and chamber heights appear positively correlated (p-value $= 9.68 \times 10^{-10}$; Pearson correlation coefficient = 0.83).

The measurements of the tortuosity show three phases as well. From chamber 1 to 16, tortuosity values are around 1. Then an important increase occurs until chamber 27, before a stabilization of tortuosity values around 3 (figure 8).

Then, we performed the same analysis in segregating between horizontal and vertical orientation of the paths. The vertical paths are mostly parallel to the roughly vertical alignment of the channels while the horizontal paths are mostly orthogonal to the main orientation of the channels. We chose the simplest criteria: if the angle between the Euclidian path (starting to ending point) and the horizontal line was more than 45°, we defined it to be vertical, or horizontal if less than 45°. Following these criteria, we found that horizontal tortuosity increases more than vertical one during shell

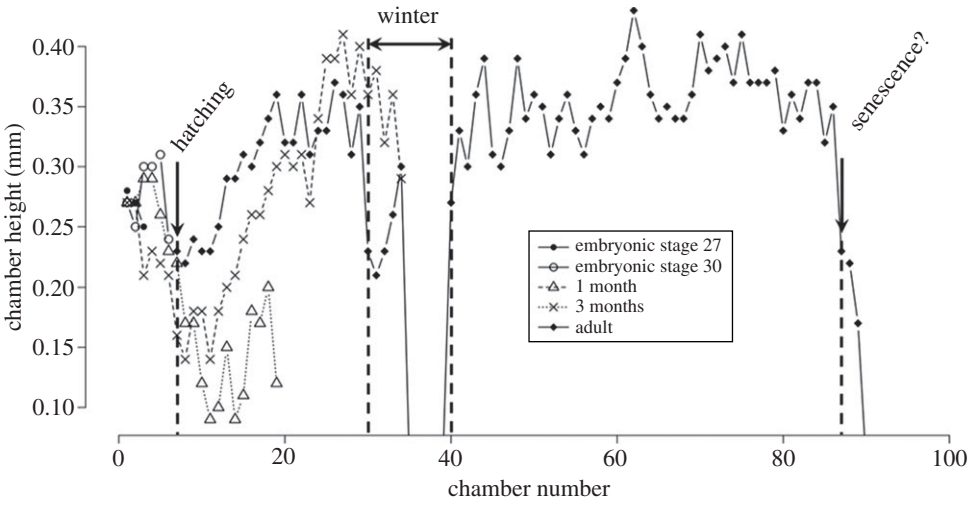

Figure 2. Chamber heights in the different studied shells (embryonic stages 27 and 30, one-month-old and three-month-old juveniles, and adult) associated with major events occurring during life cycle.

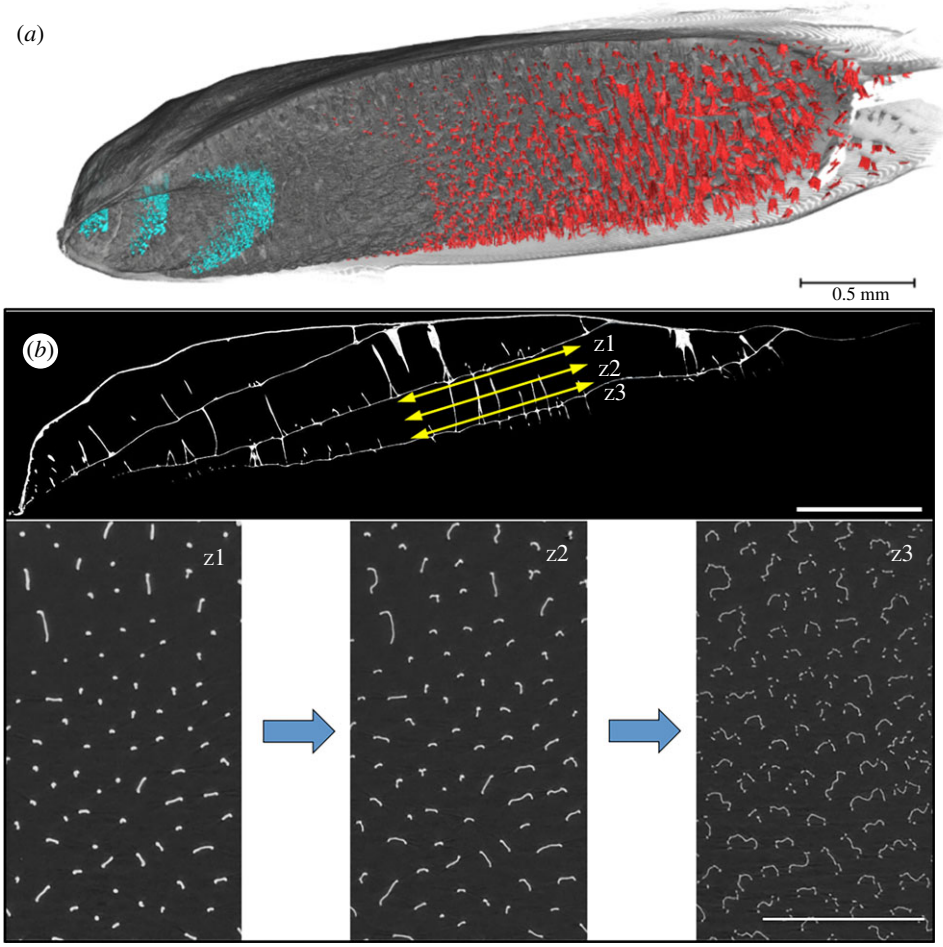

Figure 3. (*a*) Three-dimensional image of embryonic stage 27 shell ventral view with colouring of the two pillar shapes and organization area (red: 'branching' pillars; blue: 'siphuncle' pillars), and (*b*) X-ray tomography pictures of stage 27 shell illustrating the pillar shape evolution. Top picture is a sagittal plane scan along the three formed chambers with arrows z1, z2 and z3 in chamber 3 localizing (bottom pictures) the observations made from dorsal to ventral shell side. Scale bars: 0.5 mm. (Online version in colour.)

building (electronic supplementary material, figure S6). This calculation is congruent with the SEM image showing a linear pillar network structure in the shell anterior part (figure 5).

4. Discussion

Adult shell CAT-scan opens interesting prospects for the study of cuttlefish shell, and indirectly their development, ecology and evolution. Indeed, there are more than 100 cuttlefish species having various habitats (e.g. depth, temperature) and building shells with important interspecific dimorphism [21].

Our three-dimensional observations have evidenced how the cuttlebone is built and, associated with physical measurements, have revealed major changes of the shell inner structure during the first months of life of the cuttlefish.

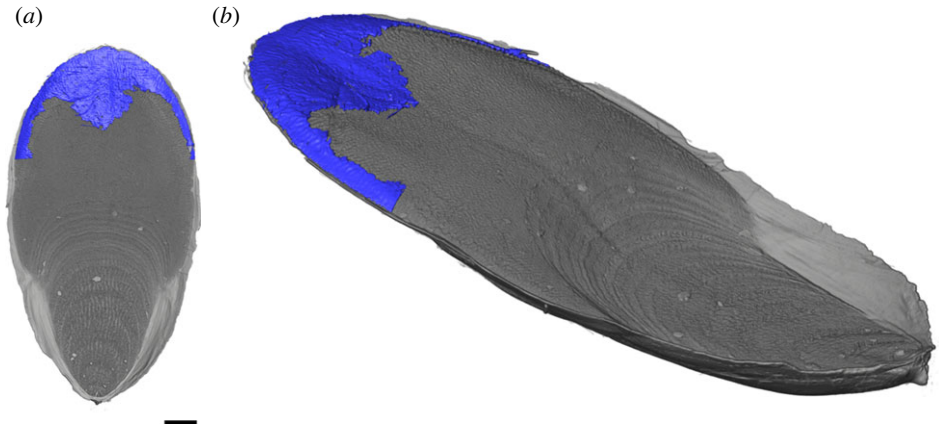

Figure 4. Three-dimensional images of one-month-old cuttlefish shell highlighting in blue the area of the new septum built from anterior to posterior: (*a*) ventral view (scale bar: 1 mm) and (*b*) ventro-lateral view. (Online version in colour.)

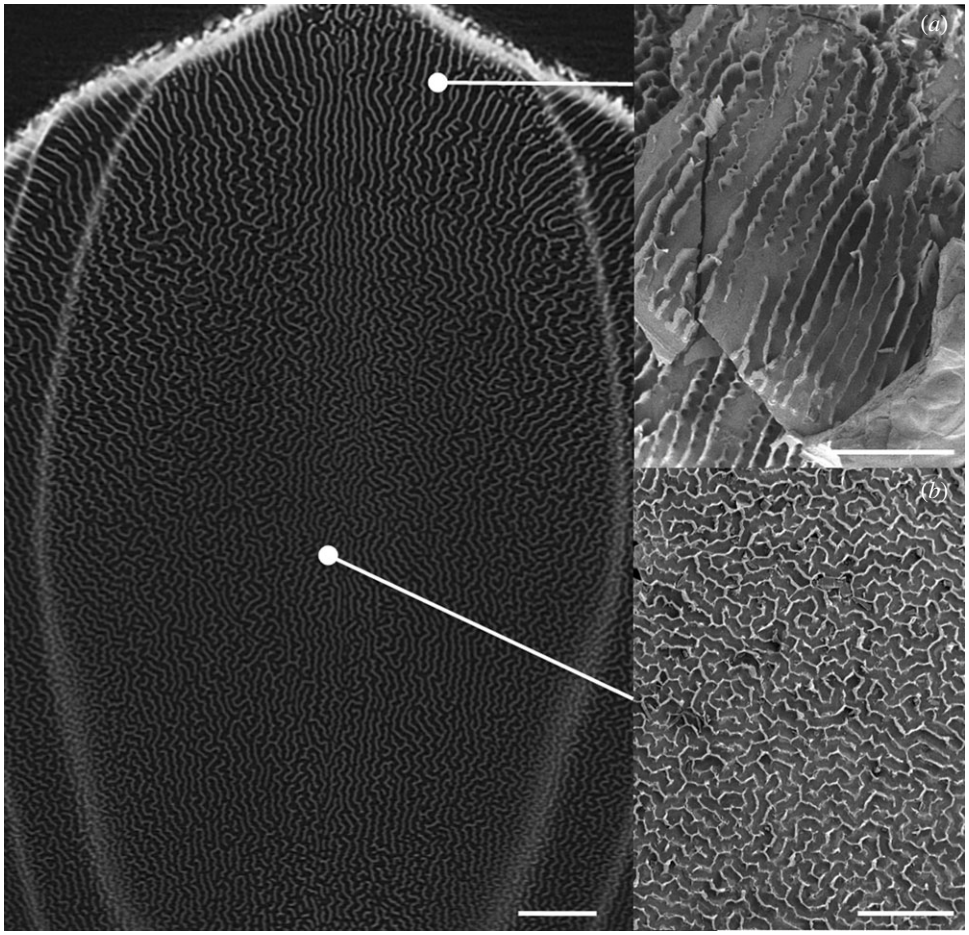

Figure 5. Labyrinthine structure of the pillar network. Left: X-ray tomography picture highlighting the pillar network organizations (30th chamber of three-month shell in top view). Right: BSE-SEM images of (*a*) a linear pillar network configuration (5 kV) found in anterior part and (*b*) a curved configuration (15 kV) found in the central chamber part. Scale bars: 1 mm.

Our results on chamber height measurements highlight some interesting variations consistent with *S. officinalis* life stages (figure 2). After hatching, juveniles stay onshore during few months to benefit from coastal prey abundance and rapid growth [22]. During this period (i.e. from 8-chamber shell), a decrease of the chamber heights in one- and three-month-old shells from animals cultured in laboratory is observed until chamber 12. This reduction can be linked with the physiological immaturity of hatchling cuttlefish. Actually, the digestive duct is still immature at least two weeks after hatching and the growth is limited [23,24]. The reduction of the chamber height could help to reduce its metabolic cost during this period, because of the high energy demand needed for other processes such as physiological adaptations to environment [14]. In the shell of adult, grown in the wild, the firstly synthetized post-hatching chambers present heights relatively constant and higher than those made in shells of reared juveniles (one- and three-month), which, according to our hypothesis, could be due to a better quality, diversity and a higher quantity of food at hatching. Indeed, the shell growth is known to depend both on the water temperature and food level [25]. After the first weeks post-hatching, the chamber heights (measured in three-month

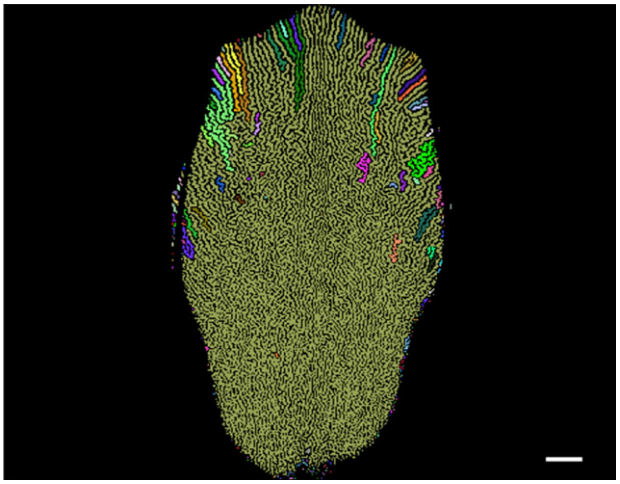

Figure 6. X-ray tomography picture of one of the last chambers (32nd chamber) of three-month shell after connectivity analysis. The different colours represent areas found to be unconnected. Scale bar: 1 mm. (Online version in colour.)

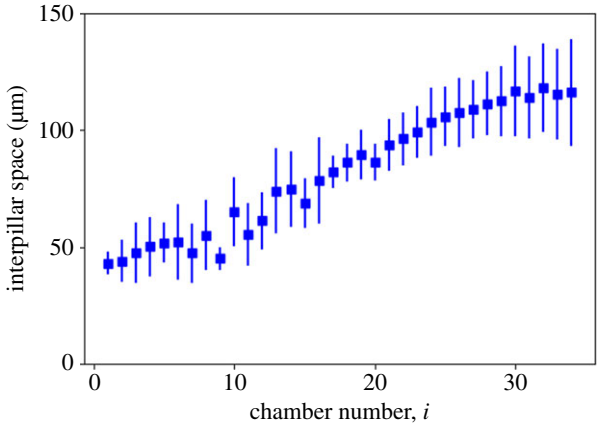

Figure 7. Graph representing the evolution of interpillar space in the different chambers of the three-month shell (mean ± standard deviation, see Material and methods). (Online version in colour.)

and adult cuttlebones) increase until chamber 20, when juvenile is mature and initiates its fast growth (figure 2). Then, the chamber heights reach values around 0.35 mm with less variability in both shells, except between the 30th and 40th chambers and after the 86th chamber (adult shell) where two important decreases are observed. This phenomenon has been previously described in cuttlefish from the English Channel as the result of animal wintering conditions [2,26], and firstly linked with slower growth due to colder temperatures and reduced feeding incurred by *Sepia officinalis* during this period of migration [14,15]. In addition, Sherrard associated also this change with depth, highlighting that cuttlebones with low chamber heights are more resistant to pressure [3]. However, the decreases observed in the three-month-old shell, as well as in the last chambers of the adult shell (around the 90th chamber), could also be the sign of the senescence of the animal, due in the first case to rearing conditions, and in the second case to the adult's end of life (cuttlefish are semelparous animals living no longer than 2 years). This smaller size is probably a consequence of the decrease in metabolism and cell activity linked to the feeding decrease of the animals [27].

By CAT-scan analysis, we confirmed that pillar growth occurs from dorsal to ventral side as previously described with microscopic observation for this species [4] and for *Sepia esculenta* [6]. During this growth, pillar shape changes

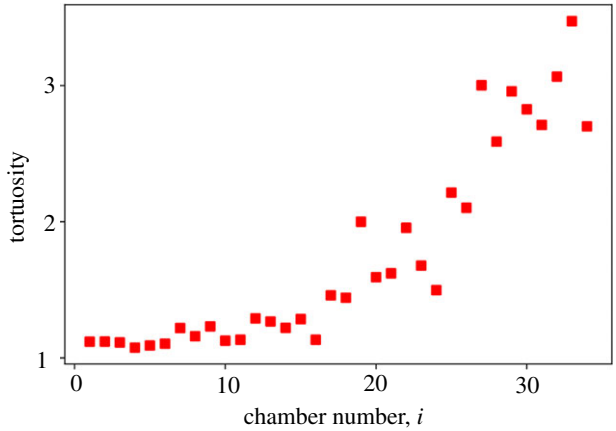

Figure 8. Graph representing the evolution of pillar network tortuosity (arithmetic mean) in the different chambers of the three-month shell. (Online version in colour.)

from a linear proximal basis to a very curved, branched distal (and apical) part. This shape change is more visible in the first formed chambers, those synthesized during embryonic period of life (figure 3) [4]. We also validated that pillars are synthesized from the anterior to the posterior part of each chamber [6], before the building of the chamber floor following the same gradient (figures 3 and 4) [3,5,7].

In addition, we evidenced a progressive linkage of the chamber pillar network resulting in a complex labyrinthine structure and determined the temporal sequence of this process. Indeed, at the end of the embryo development, in all chambers, the pillars remain isolated (i.e. the pillar network does not have a connected structure), whereas around chamber 25 the pillar network appears entirely connected. This stage is estimated to correspond to a juvenile cuttlefish between one and two months old, i.e. a few weeks before they realize an autumnal migration offshore to overwintering grounds in the deep central waters of the Channel [22]. As the pillar network constitutes a major innovation in cephalopod shell architecture by its role in avoiding implosion from hydrostatic pressure [3], we propose that the pillar network connection is a major event conferring to *S. officinalis* shell its high compressive strength, making possible migration in deeper areas.

Our interpillar space measurements are consistent with partial measurements previously done on *S. officinalis* adult shell chambers using SEM [3,28]. Nevertheless, as they are the first made on all the chambers from the same cuttlefish shell they are robust and show that there are no high variations between chambers (figure 7). Interestingly, the positive correlation found between this parameter and the chamber height indicates a co-regulation of these structural parameters involved in the cuttlebone porosity [29], but is not consistent with a shell evolution towards a higher compressive strength. However, the evolution of these two parameters (increasing until chamber 20; figures 2 and 7) associated with the complete pillar network connection (occurring around chamber 25) suggests that it is during this period that cuttlebone acquires its known mechanical properties of high porosity (93%) [30] and high compressive strength (greater than or equal to 15 atm) [31]. Although more CAT-scan analyses have to be done on pillar network at different cuttlefish life stages, our SEM personal observations on different adult cuttlebones suggest that labyrinthine structure is a homogeneous structure between different individuals.

Measurements made on the evolution of the pillar network tortuosity highlight an important change in the inner cuttlefish shell structure never shown before (figure 8). Interestingly, there is a continuous process from 'dotted' patterns at early stages to 'stripes' patterns at later stages until complete interpillar connection. The general configuration of labyrinth building, whatever the sepiid species, appears biologically controlled, but no mechanism for such a development has been proposed until now.

Regarding the role of such a structure, we propose that this structure plays a role in the buoyancy regulation of the shell. Actually, the buoyancy of *S. officinalis* has been extensively described by Denton *et al*. in the 1960s with numerous physiological experimentations [2,32–35]. They have shown that cuttlefish regulate their buoyancy by filling their cuttlebone chambers with various amount of liquid, compressing gas initially inside chambers. The amount of liquid needed to regulate the cuttlefish position in the water column is adjusted by osmotic regulation between liquid inside cuttlebone and blood vessel in direct contact with siphuncular area. Notably, they described the liquid distribution inside the different chambers: the oldest and most posterior chambers are full of liquid, the following chambers contain liquid localized on the siphuncular side, and the last synthesized 'large' chambers are full of gas. Authors explain this liquid distribution by the cuttlefish as being necessary to compensate its anterior gravity centre (with empty shell) to keep horizontal position in water without effort. However, mechanisms regulating such liquid distribution inside chambers have never been proposed. According to our observations, we propose that the labyrinthine pillar network, observed in the central chamber part from chamber 25, allows keeping liquid next to siphuncular opening in order to facilitate its input/output regulation. Actually, when the pillar network tortuosity increases, the fluid speed is expected to decrease. As the labyrinthine pillar network is mainly continuous (figure 6), the tortuosity serves to contain (or to limit) the liquid at posterior position, whereas the gas is located anteriorly. This hypothesis is consistent with the cuttlefish life cycle, which does not need to compensate great variations of hydrostatic pressure during its coastal life, whereas these variations are stronger after autumnal migration.

5. Conclusion

The non-invasive CAT-scan analysis allowed us to describe the inner structural evolution of the cuttlebone during the life cycle of *S. officinalis*. Measurements made on chamber height, interpillar space and pillar network (connection and tortuosity) highlighted important changes during the embryonic and first months of life of the cuttlefish.

The whole aspect of this structure looks clearly like typical reaction–diffusion Turing patterns with a 'dotted' to 'stripes' transition observed during the development. Such kind of transition can be obtained with a morphogen-based process that remains to be characterized.

Our observations underline the structural differences of shell chambers synthesized during embryonic, juvenile and adult stage of life. The *S. officinalis* shell seems to reach a mature cuttlebone structure (in terms of pressure resistance and porosity) around two months post-hatching. We clearly show that the pillar network, from isolated pillars first synthesized in embryos, finally form, in adult chamber shells, real walls forming a continuous labyrinth within each of the 100 chambers of the cuttlebone ventral part. We proposed that this peculiar structure has been selected as a way to control the liquid circulation and, concomitantly, the gas–liquid rate within the cuttlebone for buoyancy regulation. Associated with the hydrostatic pressure distribution role of pillars, from the last septum to internal septa, we suggest that the synthesis of such cuttlebone pillar network could correspond to a compromise between pressure compressive strength and buoyancy regulation. Finally, our results open interesting prospects to link environment, structure, function and evolution of mineralized shell, particularly unknown in extinct cephalopod species.

Ethics. Animal protocols were carried out in accordance with European legislation (directive 2010-63-UE and French decret 2013-118).

Data accessibility. Data from this study are available as electronic supplementary material.

Authors' contributions. C.L.P. designed and planned the experiment, performed data collection and analysis, as well as manuscript preparation and editing. J.D. designed and planned the mathematical and physical analyses, as well as manuscript editing. G.L. performed data analysis and manuscript editing. P.-J.L. and L.B.-P. wrote the project, supervised the experiments, and assisted with the data interpretation and manuscript editing. All authors gave final approval for publication and agree to be held accountable for the work performed therein.

Competing interests. The authors have no competing interests.

Funding. This work was supported by ATM 'Minéral-Vivant', Museum National d'Histoire Naturelle.

Acknowledgements. CAT-scan was performed at the AST-RX platform of the MNHN with the help of P. Wills, and SEM analysis on the Electronic Microscopy Technical Platform of the MNHN with the help of G. Toutirais. We thank C. Jozet-Alves and the CREC (University of Caen) for providing shells of juveniles, and J.-P. Robin for obtaining adult cuttlefish in fish market of Port-en-Bessin-Huppain.

References

1. Denton EJ. 1974 On buoyancy and the lives of modern and fossil cephalopods. *Proc. R. Soc. Lond. B* **185**, 273–299. (doi:10.1098/rspb.1974.0020)
2. Denton EJ, Gilpin-Brown JB. 1961 The buoyancy of the cuttlefish, *Sepia officinalis* (L.). *J. Mar. Biol. Assoc. UK* **41**, 319–342. (doi:10.1017/S0025315400023948)
3. Sherrard KM. 2000 Cuttlebone morphology limits habitat depth in eleven species of *Sepia* (Cephalopoda: Sepiidae). *Biol. Bull.* **198**, 404–414. (doi:10.2307/1542696)
4. Le Pabic C, Rousseau M, Bonnaud-Ponticelli L, von Boletzky S. 2016 Overview of the shell development of the common cuttlefish *Sepia officinalis* during early-life stages. *Vie Milieu - Life Environ.* **66**, 35–42.
5. Bandel K, von Boletzky S. 1979 A comparative study of the structure, development and morphological relationships of chambered cephalopod shells. *The Veliger* **21**, 313–354.
6. Tanabe K, Fukuda Y, Ohtsuka Y. 1985 New chamber formation in the cuttlefish *Sepia esculenta* Hoyle. *Venus* **44**, 55–67.
7. Checa AG, Cartwright JHE, Sánchez-Almazo I, Andrade JP, Ruiz-Raya F. 2015 The cuttlefish *Sepia officinalis* (Sepiidae, Cephalopoda) constructs cuttlebone from a liquid-crystal precursor. *Sci. Rep.* **5**, 11513. (doi:10.1038/srep11513)
8. Čadež V, Škapin SD, Leonardi A, Križaj I, Kazazić S, Salopek-Sondi B, Sondi I. 2017 Formation and

morphogenesis of a cuttlebone's aragonite biomineral structures for the common cuttlefish (*Sepia officinalis*) on the nanoscale: revisited. *J. Colloid Interface Sci.* **508**, 95–104. (doi:10.1016/j.jcis.2017.08.028)

9. Le Pabic C, Marie A, Marie B, Percot A, Bonnaud-Ponticelli L, Lopez PJ, Luquet G. 2017 First proteomic analyses of the dorsal and ventral parts of the *Sepia officinalis* cuttlebone. *J. Proteomics* **150**, 63–73. (doi:10.1016/j.jprot.2016.08.015)
10. Lemaire J. 1970 Table de développement embryonnaire de *Sepia officinalis* L. (Mollusque, Céphalopode). *Bull. Soc. Zool. Fr.* **95**, 773–782.
11. Oestmann DJ, Scimeca JM, Forsythe J, Hanlon RT, Lee P. 1997 Special considerations for keeping cephalopods in laboratory facilities. *J. Am. Assoc. Lab. Anim. Sci.* **36**, 89–93.
12. Sykes AV, Baptista FD, Gonçalves RA, Andrade JP. 2012 Directive 2010/63/EU on animal welfare: a review on the existing scientific knowledge and implications in cephalopod aquaculture research. *Rev. Aquac.* **4**, 142–162. (doi:10.1111/j.1753-5131.2012.01070.x)
13. Butler-Struben HM, Brophy SM, Johnson NA, Crook RJ. 2018 *In vivo* recording of neural and behavioral correlates of anesthesia induction, reversal, and euthanasia in cephalopod molluscs. *Front. Physiol.* **9**, 109. (doi:10.3389/fphys.2018.00109)
14. von Boletzky S. 1974 Effets de la sous-nutrition prolongée sur le développement de la coquille de *Sepia officinalis* L. (Mollusca, Cephalopoda). *Bull. Soc. Zool. Fr.* **99**, 667–673.
15. Richard A. 1969 The part played by temperature in the rhythm of formation of markings on the shell of cuttlefish *Sepia officinalis* (Cephalopoda, Mollusca). *Experientia* **25**, 1051–1052. (doi:10.1007/BF01901423)
16. van der Walt S, Schönberger JL, Nunez-Iglesias J, Boulogne F, Warner JD, Yager N, Gouillart E, Yu T, the scikit-image Contributors. 2014 scikit-image: image processing in Python. *PeerJ* **2**, e453. (doi:10.7717/peerj.453)
17. Fiorio C, Gustedt J. 1996 Two linear time union-find strategies for image processing. *Theor. Comput. Sci.* **154**, 165–181. (doi:10.1016/0304-3975(94)00262-2)
18. Wu K, Otoo E, Shoshani A. 2005 Optimizing connected component labeling algorithms. *Proc. SPIE Conf. Med. Imag.* **5747**, 1965–1976. (doi:10.1117/12.596105)
19. Otsu N. 1979 A threshold selection method from gray-level histograms. *IEEE Trans. Syst. Man. Cybern.* **9**, 62–66. (doi:10.1109/TSMC.1979.4310076)
20. Dijkstra EW. 1971 *A short introduction to the art of programming*. Eindhoven, The Netherlands: Technical University Editor.
21. Adam W, Rees WJ. 1966 *A review of the cephalopod family Sepiidae*. London, UK: British Museum-Natural History Editor.
22. Bloor ISM, Attrill MJ, Jackson EL. 2013 A review of the factors influencing spawning, early life stage survival and recruitment variability in the common cuttlefish (*Sepia officinalis*). *Adv. Mar. Biol.* **65**, 1–65. (doi:10.1016/B978-0-12-410498-3.00001-X)
23. Yim M, Boucaud-Camou E. 1980 Etude cytologique du développement post-embryonnaire de la glande digestive de *Sepia officinalis* L. (Mollusque Céphalopode). *Arch. Anat. Microsc. Morphol. Exp.* **69**, 59–79. (doi:10.1139/f93-063)
24. Le Pabic C, Caplat C, Lehodey J-P, Dallas L, Koueta N. 2015 Physiological perturbations in juvenile cuttlefish *Sepia officinalis* induced by subchronic exposure to dissolved zinc. *Mar. Pollut. Bull.* **95**, 678–687. (doi:10.1016/j.marpolbul.2015.02.018)
25. Martínez P, Bettencourt V, Guerra Á, Moltschaniwskyj NA. 2000 How temperature influences muscle and cuttlebone growth in juvenile cuttlefish (*Sepia elliptica*) (Mollusca: Cephalopoda) under conditions of food stress. *Can. J. Zool.* **78**, 1855–1861. (doi:10.1139/z00-115)
26. Hewitt RA, Stait B. 1988 Seasonal variation in septal spacing of *Sepia officinalis* and some Ordovician actinocerid nautiloids. *Lethaia* **21**, 383–394. (doi:10.1111/j.1502-3931.1988.tb01767.x)
27. Boletzky SV. 1974 Effets de la sous-nutrition prolongée sur le développement de la coquille de *Sepia officinalis* L. (Mollusca, Cephalopoda). *Bull. Soc. Zool. Fr.* **99**, 667–673.
28. Florek M, Fornal E, Gómez-Romero P, Zieba E, Paszkowicz W, Lekki J, Nowak J, Kuczumow A. 2009 Complementary microstructural and chemical analyses of *Sepia officinalis* endoskeleton. *Mater. Sci. Eng. C* **29**, 1220–1226. (doi:10.1016/j.msec.2008.09.040)
29. Gutowska MA, Melzner F, Pörtner HO, Meier S. 2010 Cuttlebone calcification increases during exposure to elevated seawater pCO_2 in the cephalopod *Sepia officinalis*. *Mar. Biol.* **157**, 1653–1663. (doi:10.1007/s00227-010-1438-0)
30. Birchall JD, Thomas NL. 1983 On the architecture and function of cuttlefish bone. *J. Mater. Sci.* **18**, 2081–2086. (doi:10.1007/BF00555001)
31. Ward PD, von Boletzky S. 1984 Shell implosion depth and implosion morphologies in three species of *Sepia* (Cephalopoda) from the Mediterranean Sea. *J. Mar. Biol. Assoc. UK* **64**, 955–966. (doi:10.1017/S0025315400047366)
32. Denton EJ, Gilpin-Brown JB. 1959 Buoyancy of the cuttlefish. *Nature* **184**, 1330–1331. (doi:10.1038/1841330a0)
33. Denton EJ, Gilpin-Brown JB. 1961 The effect of light on the buoyancy of the cuttlefish. *J. Mar. Biol. Assoc. UK* **41**, 343–350. (doi:10.1017/S002531540002395X)
34. Denton EJ, Gilpin-Brown JB. 1961 The distribution of gas and liquid within the cuttlebone. *J. Mar. Biol. Assoc. UK* **41**, 365–381. (doi:10.1017/S0025315400023973)
35. Denton EJ, Gilpin-Brown JB, Howarth JV. 1961 The osmotic mechanism of the cuttlebone. *J. Mar. Biol. Assoc. UK* **41**, 351–364. (doi:10.1017/S0025315400023961)